Inorg. Chem. **2006**, *45*, 8711–8718

Inorganic Chemistry

Article

Homoleptic Zinc(II) Complexes with First and Second Coordination Shells of 5-*tert*-Butylpyrazole

Sylvie L. Renard, Isabelle Sylvestre, Simon A. Barrett, Colin A. Kilner, and Malcolm A. Halcrow*

School of Chemistry, University of Leeds, Woodhouse Lane, Leeds LS2 9JT, U.K.

Received December 16, 2005

Reaction of hydrated $Zn[NO_3]_2$ or $Zn[BF_4]_2$ with four or more equivalents of 3{5}-*tert*-butylpyrazole (L^{tBu}) yields $[Zn(L^{tBu})_4]X_2$ ($X^- = NO_3^-$ or BF_4^-). The nitrate complex contains C_2-symmetric four-coordinate zinc(II) centers with a slightly flattened tetrahedral geometry, and each nitrate anion hydrogen bonds to two pyrazole N–H groups. Similar reactions with $Zn[ClO_4]_2$ or $ZnCl_2$ in the presence of 2 equiv of $AgPF_6$ or $AgSbF_6$ yield instead $[\{Zn(L^{tBu})_4\}(L^{tBu})_4][ClO_4]_2$ and $[\{Zn(L^{tBu})_4\}(L^{tBu})_2]Y_2$ ($Y^- = PF_6^-$ or SbF_6^-). Crystals of $[\{Zn(L^{tBu})_4\}(L^{tBu})_4][ClO_4]_2$ are composed of discrete $[\{Zn(L^{tBu})_4\}(L^{tBu})_4]^{2+}$ supramolecules that are formed from N–H···N hydrogen bonding between zinc-bound and uncoordinated pyrazole rings. The $[\{Zn(L^{tBu})_4\}(L^{tBu})_4]^{2+}$ moieties are linked into planar 4^4 nets by hydrogen bonding to bridging ClO_4^- anions. The ClO_4^- ions are almost perfectly encapsulated in near-spherical cavities of approximate dimensions 5.0 × 5.0 × 4.5 Å that are formed by two interlocked supramolecular dications. Similarly, $[\{Zn(L^{tBu})_4\}(L^{tBu})_2][PF_6]_2$ crystallizes as discrete supramolecules in the crystal with the PF_6^- anions occupying a shallow bowl-shaped cavity on the surface of the complex that is formed by two zinc-bound and one uncoordinated pyrazole ligands. ^1H NMR and IR studies of $[\{Zn(L^{tBu})_4\}(L^{tBu})_4][ClO_4]_2$ in CD_2Cl_2 imply that the second-sphere L^{tBu} ligands dissociate from the $[Zn(L^{tBu})_4]^{2+}$ center in this solvent and that free and metal-bound L^{tBu} are in rapid chemical exchange.

Introduction

Ligands that can simultaneously bind cations and anions are of increasing interest to coordination and supramolecular chemists[1] for their potential applications in anion sensing,[2] hydrometallurgy,[3] and waste treatment. We[4−8] and others[9−12] have found that the pyrazole ring is a powerful ditopic receptor for metal cations (through its pyridinic N atom) and anions (via the pyrrolic N−H group). During our own work, we have reported that the $[ZnX(L^{tBu})_3]^+$ ($X^- = Cl^-$, Br^-, or I^-; L^{tBu} = 5-*tert*-butylpyrazole, Chart 1) cation presents a bowl-shaped cavity on one face of the tetrahedral molecule, which is formed from the *tert*-butyl substituents with the three pyrazole N−H groups at its center.[7] This cavity can bind a range of anions in the solid state and in weakly polar solvents that range in size from halides up to globular

---

* To whom correspondence should be addressed. E-mail: m.a.halcrow@leeds.ac.uk.

(1) For selected recent examples see: (a) Glenny, M. W.; Blake, A. J.; Wilson, C.; Schröder, M. *Dalton Trans.* **2003**, 1941. (b) Plieger, P. G.; Tasker, P. A.; Galbraith, S. G. *Dalton Trans.* **2004**, 313. (c) Bondy, C. R.; Gale, P. A.; Loeb, S. J. *J. Am. Chem. Soc.* **2004**, *126*, 5030. (d) Harding, L. P.; Jeffery, J. C.; Riis-Johannessen, T.; Rice, C. R.; Zeng, Z. *Chem. Commun.* **2004**, 654. (e) Gunning, P.; Benniston, A. C.; Peacock, R. D. *Chem. Commun.* **2004**, 2226. (f) Koskela, S. J. M.; Fyles, T. M.; James, T. D. *Chem. Commun.* **2005**, 945. (g) Curiel, D.; Beer, P. D. *Chem. Commun.* **2005**, 1909. (h) Vega, I. E.; Gale, P. A.; Light, M. E.; Loeb, S. J. *Chem. Commun.* **2005**, 4913. (i) Duckmanton, P. A.; Blake, A. J.; Love, J. B. *Inorg. Chem.* **2005**, *44*, 7708. (j) Pask, C. M.; Camm, K. D.; Bullen, N. J.; Carr, M. J.; Clegg, W.; Kilner, C. A.; Halcrow, M. A. *Dalton Trans.* **2006**, 662.

(2) (a) Beer, P. D.; Hayes, E. J. *Coord. Chem. Rev.* **2003**, *240*, 167. (b) Beer, P. D.; Bayly, S. R. *Top. Curr. Chem.* **2005**, *255*, 125.

(3) Galbraith, S. G.; Tasker, P. A. *Supramol. Chem.* **2005**, *17*, 191.

(4) (a) Liu, X.; McAllister, J. A.; de Miranda, M. P.; Whitaker, B. J.; Kilner, C. A.; Thornton-Pett, M.; Halcrow, M. A. *Angew. Chem., Int. Ed.* **2002**, *41*, 756. (b) Liu, X.; McAllister, J. A.; de Miranda, M. P.; McInnes, E. J. L.; Kilner, C. A.; Halcrow, M. A. *Chem.*—*Eur. J.* **2004**, *10*, 1827.

(5) Liu, X.; McLaughlin, A. C.; de Miranda, M. P.; McInnes, E. J. L.; Kilner, C. A.; Halcrow, M. A. *Chem. Commun.* **2002**, 2978.

(6) Liu, X.; de Miranda, M. P.; McInnes, E. J. L.; Kilner, C. A.; Halcrow, M. A. *Dalton Trans.* **2004**, 59.

(7) (a) Liu, X.; Kilner, C. A.; Halcrow, M. A. *Chem. Commun.* **2002**, 704. (b) Renard, S. L.; Kilner, C. A.; Fisher, J.; Halcrow, M. A. *J. Chem. Soc., Dalton Trans.* **2002**, 4206.

(8) Renard, S. L.; Franken, A.; Kilner, C. A.; Kennedy, J. D.; Halcrow, M. A. *New J. Chem.* **2002**, *26*, 1634.

(9) Looney, A.; Parkin, G.; Rheingold, A. L. *Inorg. Chem.* **1991**, *30*, 3099.

(10) Reger, D. L.; Ding, Y.; Rheingold, A. L.; Ostrander, R. L. *Inorg. Chem.* **1994**, *33*, 4226.

(11) Nieto, S.; Pérez, J.; Riera, V.; Miguel, D.; Alvarez, C. *Chem. Commun.* **2005**, 546.

(12) Onishi, M.; Yamaguchi, M.; Kumagae, S.; Kawano, H.; Arikawa, Y. *Inorg. Chim. Acta* **2006**, *359*, 990.

10.1021/ic052144q CCC: $33.50

Chart 1. Pyrazole Ligands Used in This Work and the Abbreviations Applied to Them in the Text

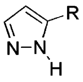

L^R

carborane derivatives.[7,8] Related bowl-shaped anion receptors formed from other metal trispyrazolyl hosts also have been prepared by others.[9−12] As a continuation of this work, we looked forward to seeing what structural motifs would arise from the complexation of a zinc(II) salt of a weakly coordinating anion with L^{tBu} in the absence of halide. Here, we report five complex salts of type $[Zn(L^{tBu})_4]X_2$, at least two of which interact with additional molecules of L^{tBu} in the solid state to form extended supramolecular host cavities for their anions. These are the first crystallographically characterized $[M(pz)_4]X_2$ (pz = a monodentate pyrazole derivative, X^- = an anion) derivatives for M = Zn, although this stoichiometry of complex is very well-known in the chemistry of other transition ions.[13−23]

Experimental Section

General Information. All manipulations were performed in air using commercial grade solvents. 3{5}-*tert*-butylpyrazole (L^{tBu}),[24] 3{5}-(thien-2-yl)pyrazole (L^{Tn}),[25] 3{5}-*iso*propylpyrazole (L^{iPr}),[26] and 3{5}-(2,4,6-trimethylphenyl)pyrazole (L^{Mes})[27] were prepared by the literature procedures, while all other reagents were purchased commercially and used as supplied. [***Caution:*** *While we have not experienced any difficulty in handling* $[\{Zn(L^{tBu})_4\}(L^{tBu})_4][ClO_4]_2$ ***(3)***, *metal-organic perchlorates are potentially explosive and should be handled with due care in small quantities*].

Electrospray (ES) (MeCN matrix) mass spectrometry (MS) was performed with a Micromass LCT time-of-flight spectrometer. All quoted peaks have the correct isotopic distribution for their proposed assignments. Carbon−hydrogen−nitrogen (CHN) microanalyses were performed by the University of Leeds School of Chemistry microanalytical service. Nuclear magnetic resonance (NMR) spectra were run on a Bruker DRX500 spectrometer, which operates at 500.1 MHz (^1H) and 125.8 MHz (^{13}C). Infrared (IR) spectra were run as Nujol mulls pressed between NaCl plates (or in NaCl solution cells) using a Nicolet Avatar 360 spectrophotometer. Powder diffraction data were obtained with a PANalytical X'Pert MPD diffractometer using Cu radiation (λ = 1.5418 Å).

Synthesis of $[Zn(L^{tBu})_4][NO_3]_2$ (1) and $[Zn(L^{tBu})_4][BF_4]_2$ (2). Compound **1** was prepared by stirring $Zn[NO_3]_2{\cdot}6H_2O$ (0.24 g, 0.81 mmol) with 3{5}-*tert*-butylpyrazole (0.40 g, 3.2 mmol) in MeOH (25 cm^3) at room temperature until all the solid had dissolved (ca. 15 min). Evaporation of the solution initially yielded a colorless oil, which slowly converted to a white solid residue upon further heating to 60 °C in vacuo (it is important that complete removal of the methanol solvent is achieved). This solid was redissolved in the minimum volume of CH_2Cl_2 and filtered. Approximately 5 times the volume of pentane was added to the solution, which was stored overnight at 5 °C to yield colorless crystals that were isolated, washed with pentane, and dried in vacuo. Yield 0.24 g, 44%. An identical reaction employing $Zn[BF_4]_2{\cdot}6H_2O$ (0.28 g, 0.81 mmol) gave **2** as large colorless prisms that decomposed rapidly to a white powder upon exposure to air. Yield 0.31 g, 52%.

For **1**, found: C, 48.6; H, 7.1; N, 20.4. Anal. Calcd for $C_{28}H_{48}N_{10}O_6Zn$: C, 49.0; H, 7.1; N, 20.4. ESMS: *m/z* 270 $[^{64}Zn(L^{tBu})(NCMe)_2]^+$, 312 $[^{64}Zn(L^{tBu})_2]^+$, 332 $[^{64}Zn(L^{tBu})(NCMe)_2(NO_3)]^+$, 353 $[^{64}Zn(L^{tBu})_2(NCMe)]^+$, 374 $[^{64}Zn(L^{tBu})_2(NO_3)]^+$, 394 $[^{64}Zn(L^{tBu})_2(NCMe)_2]^+$, 415 $[^{64}Zn(L^{tBu})_2(NCMe)(NO_3)]^+$, 417 $[^{64}Zn_2(L^{tBu})_2(NCMe)]^+$, 500 $[^{64}Zn_2(L^{tBu})_3]^+$, 520 $[^{64}Zn_2(L^{tBu})_2(NCMe)_2(NO_3)]^+$, 541 $[^{64}Zn_2(L^{tBu})_2(NCMe)(NO_3)_2]^+$. NMR spectra ($CDCl_3$, 295 K) ^1H δ (ppm): 1.27 (36H, CCH_3), 6.21 (d, 2.2 Hz, 4H, Pz H^4), 7.71 (d, 2.2 Hz, 4H, Pz H^3), 11.66 (br s, 4H, N*H*). $\{^1H\}^{13}C$ δ (ppm): 30.3 (CCH_3), 31.7 (CCH_3), 103.1 (Pz C^4), 140.4 (Pz C^3), 156.9 (Pz C^5). IR (Nujol): 3170m, 3134m, 1567m, 1489m, 1354m, 1321s, 1279s, 1210m, 1175w, 1121s, 1033m, 992s, 963s, 941m, 888w, 808m, 722w, 665w, 642w cm^{-1}. IR (CD_2Cl_2): 3470w, 3210m cm^{-1}.

For **2,** found: C, 46.1; H, 6.7; N, 15.4. Anal. Calcd for $C_{28}H_{48}B_2F_8N_8Zn$: C, 45.7; H, 6.6; N, 15.2. ESMS: *m/z* 270 $[^{64}Zn(L^{tBu})(NCMe)_2]^+$, 312 $[^{64}Zn(L^{tBu})_2]^+$, 353 $[^{64}Zn(L^{tBu})_2(NCMe)]^+$, 394 $[^{64}Zn(L^{tBu})_2(NCMe)_2]^+$, 417 $[^{64}Zn_2(L^{tBu})_2(NCMe)]^+$, 477 $[^{64}Zn_2(L^{tBu})_2(NCMe)_2F]^+$, 500 $[^{64}Zn_2(L^{tBu})_3]^+$. NMR spectra ($CDCl_3$, 295 K) ^1H δ (ppm): 1.28 (36H, CCH_3), 6.20 (d, 2.1 Hz, 4H, Pz H^4), 7.74 (d, 2.1 Hz, 4H, Pz H^3), 9.55 (br s, 4H, N*H*). $\{^1H\}^{13}C$ δ (ppm): 30.1 (CCH_3), 31.7 (CCH_3), 103.4 (Pz C^4), 141.6 (Pz C^3),

---

(13) Reedijk, J. *Recl. Trav. Chim. Pays-Bas* **1969**, *88*, 1451.

(14) (a) Reedijk, J. *Recl. Trav. Chim. Pays-Bas* **1970**, *89*, 605. (b) Reedijk, J.; Windhorst, J. C. A.; van Ham, N. H. M.; Groeneveld, W. L. *Recl. Trav. Chim. Pays-Bas* **1971**, *90*, 234.

(15) For examples, see: (a) Mighell, A.; Santoro, A.; Prince, E.; Reimann, C. *Acta Crystallogr., Sect. B* **1975**, *B31*, 2479. (b) Kogane, T.; Ishii, M.; Harada, K.; Hirota, R.; Nakahara, M. *Bull Chem. Soc. Jpn.* **1989**, *62*, 2524. (c) Liu, X.; Kilner, C. A.; Thornton-Pett, M.; Halcrow, M. A. *Acta Crystallogr., Sect. C* **2001**, *C57*, 1253. (d) Malecka, M.; Checinska, L. *Acta Crystallogr., Sect. C* **2003**, *C59*, m115.

(16) (a) Sakai, K.; Yamada, Y.; Tsubomura, T.; Yabuki, M.; Yamaguchi, M. *Inorg. Chem.* **1996**, *35*, 542. (b) Sun, Y.-J.; Cheng, P.; Yan, S.-P.; Liao, D.-Z.; Jiang, Z.-H.; Shen, P.-W. *J. Mol. Struct.* **2001**, *597*, 191.

(17) For examples, see: (a) Mighell, A. D.; Reimann, C. W.; Santoro, A. *Acta Crystallogr., Sect. B* **1969**, *B25*, 595. (b) Helmholdt, R. B.; Hinrichs, W.; Reedijk, J. *Acta Crystallogr., Sect. C* **1987**, *C43*, 226. (c) Hvastijova, M.; Kohout, J.; Diaz, J. G.; Kozisek, J.; Buchler, J. W. *Transition Met. Chem.* **2001**, *26*, 430. (d) Nelana, S. M.; Darkwa, J.; Guzei, I. A.; Mapolie, S. F. *J. Organomet. Chem.* **2004**, *689*, 1835.

(18) Chen, X.; Du, J.-Y.; Shi, H.-Q. *Pol. J. Chem.* **2000**, *74*, 889. (b) Sun, Y.-J.; Chen, X.-Y.; Cheng, P.; Yan, S.-P.; Liao, D.-Z.; Jiang, Z.-H.; Shen, P.-W. *J. Mol. Struct.* **2002**, *613*, 167.

(19) (a) Egan, J. W.; Theopold, K. H. *Acta Crystallogr., Sect. C* **1990**, *C46*, 1013. (b) Hong, C. S.; Koo, J.-E.; Son, S.-K.; Lee, Y. S.; Kim, Y.-S.; Do, Y. *Chem.*−*Eur. J.* **2001**, *7*, 4243. (c) Hvastijová, M.; Bočba, R.; Kohout, J.; Jäger, L.; Císařová, I.; Kožíšek, J. *Inorg. Chim. Acta* **2003**, *343*, 217.

(20) (a) Dittmar, H.; Bohn, K.; Walker, N. *Z. Kristallogr.* **2000**, *215*, 189. (b) Cotton, S. A.; Franckevicius, V.; Fawcett, J. *Polyhedron* **2002**, *21*, 2055. (c) Ganesan, P. V.; Kepert, C. J. *Chem. Commun.* **2004**, 2168.

(21) (a) Chen, J.; Woo, L. K. *Polyhedron* **1999**, *18*, 825. (b) Graziani, O.; Toupet, L.; Hamon, J.-R.; Tilset, M. *Inorg. Chim. Acta* **2002**, *341*, 127.

(22) For examples, see: (a) Reedijk, J.; Storke-Blaise, B. A.; Verschoor, G. C. *Inorg. Chem.* **1971**, *10*, 2594. (b) Lumme, P.; Mutikainen, I.; Lindell, E. *Inorg. Chim. Acta* **1987**, *217*, 71. (c) Lumme, P. O.; Lindell, E.; Mutikainen, I. *Acta Crystallogr., Sect. C* **1988**, *C44*, 967. (d) Goher, M. A. S.; Mautner, F. A.; Abu-Youssef, M. A. M. *Transition Met. Chem.* **1999**, *24*, 29.

(23) For examples, see: (a) Dapporto, P.; Mani, F. *J. Chem. Res., Miniprint* **1979**, 4201. (b) Pieper, T.; Sommer, M.; Galanski, M.; Keppler, B. K.; Giester, G. *Z. Anorg. Allg. Chem.* **2001**, *627*, 261. (c) Pruchnik, F. P.; Jakimowicz, P.; Ciunik, Z.; Zakrzewska-Czerwińska, J.; Opolski, A.; Wietrzyk, J.; Wojdat, E. *Inorg. Chim. Acta* **2002**, *334*, 59. (d) Mayboroda, A.; Rheinwald, G.; Lang, H. *Inorg. Chim. Acta* **2003**, *355*, 69.

(24) Trofimenko, S.; Calabrese, J. C.; Thompson, J. S. *Inorg. Chem.* **1987**, *26*, 1507.

(25) Calabrese, J. C.; Domaille, P. J.; Trofimenko, S.; Long, G. J. *Inorg. Chem.* **1991**, *30*, 2795.

(26) Trofimenko, S.; Calabrese, J. C.; Domaille, P. J.; Thompson, J. S. *Inorg. Chem.* **1989**, *28*, 1091.

(27) Rheingold, A. L.; White, C. B.; Trofimenko, S. *Inorg. Chem.* **1993**, *32*, 3471.

157.4 (Pz C^5). IR (Nujol): 3258m, 3161w, 3129m, 1566m, 1490m, 1338w, 1306m, 1259m, 1212m, 1177w, 1123s, 1090s br, 1025m, 1008m, 990m, 973m, 961s, 902w, 843m, 803m, 761w, 723w, 665w, 641w cm^{-1}. IR (CD_2Cl_2): 3470w, 3331m cm^{-1}.

Synthesis of [{Zn(L^{tBu})$_4$}(L^{tBu})$_4$][ClO$_4$]$_2$ (3). Zn[ClO$_4$]$_2$·6H$_2$O (0.26 g, 0.71 mmol) and 3{5}-*tert*-butylpyrazole (0.70 g, 5.6 mmol) were stirred in MeOH (25 cm^3) at room temperature until all the solid had dissolved. Evaporation and recrystallization from CH_2Cl_2/pentane, as for **1**, yielded large colorless cubic crystals of **3**. Yield 0.24 g, 38%. Analytical data. Found: C, 53.2; H, 7.8; N, 18.0. Anal. Calcd for $C_{56}H_{96}Cl_2N_{16}O_8Zn$: C, 53.5; H, 7.7; N, 17.8. ESMS: *m*/*z* 125 [L^{tBu} + H]$^+$, 270 [^{64}Zn(L^{tBu})(NCMe)$_2$]$^+$, 312 [^{64}Zn(L^{tBu})$_2$]$^+$, 353 [^{64}Zn(L^{tBu})$_2$(NCMe)]$^+$, 394 [^{64}Zn(L^{tBu})$_2$(NCMe)$_2$]$^+$, 417 [^{64}Zn$_2$(L^{tBu})$_2$(NCMe)]$^+$, 452 [^{64}Zn(L^{tBu})$_2$(NCMe)(^{35}ClO$_4$)]$^+$, 500 [^{64}Zn$_2$(L^{tBu})$_3$]$^+$, 557 [^{64}Zn$_2$(L^{tBu})$_2$(NCMe)$_2$(^{35}ClO$_4$)]$^+$, 574 [^{64}Zn$_2$(L^{tBu})$_2$(^{35}ClO$_4$)$_2$]$^+$. NMR spectra (CDCl$_3$, 295 K) ^{1}H δ (ppm): 1.26 (72H, CCH_3), 6.10 (d, 2.1 Hz, 8H, Pz H^4), 7.32 (d, 2.1 Hz, 8H, Pz H^3), 11.22 (br s, 8H, NH). {^{1}H}^{13}C δ (ppm): 30.4 (CCH$_3$), 31.7 (CCH$_3$), 102.7 (Pz C^4), 138.7 (Pz C^3), 157.6 (Pz C^5). IR (Nujol): 3327s, 3170w, 3146m, 3099m, 3069w, 1582w, 1563m, 1488m, 1338w, 1309s, 1258m, 1209m, 1174w, 1106s br, 1053m, 995s, 961s, 934m, 871w, 805m, 782s, 725m, 684w, 665w, 639w, 624m cm^{-1}. IR (CD_2Cl_2): 3470m, 3257m cm^{-1}.

Synthesis of [{Zn(L^{tBu})$_4$}(L^{tBu})$_2$][PF$_6$]$_2$ (4) and [{Zn(L^{tBu})$_4$}(L^{tBu})$_2$][SbF$_6$]$_2$ (5). Compound **4** was synthesized as follows. A mixture of ZnCl$_2$ (0.11 g, 0.81 mmol), 3{5}-*tert*-butylpyrazole (0.60 g, 4.8 mmol), and AgPF$_6$ (0.41 g, 1.6 mmol) in MeOH (25 cm^3) was stirred at room temperature for 16 h. The resultant colorless solution was filtered and evaporated to dryness, leaving an oily residue. This was redissolved in the minimum volume of CH$_2$Cl$_2$, filtered, and diluted with ca. twice the volume of pentane. Overnight storage of the solution at 5 °C gave colorless hexagonal crystals that were isolated, washed with pentane, and dried in vacuo. Yield 0.29 g, 33%. An identical reaction employing AgSbF$_6$ (0.55 g, 1.6 mmol) gave colorless crystals of **5** that had the same hexagonal habit as **4** but experienced twinning. These crystals were stable under their mother liquor but decomposed upon direct exposure to air at room temperature, yielding a white, sticky solid that was analyzed approximately as the monohydrate of **5**. All characterization was carried out using this material.

For **4**, found: C, 45.8; H, 6.7; N, 15.4. Anal. Calcd for $C_{42}H_{72}F_{12}N_{12}P_2Zn$: C, 45.8; H, 6.6; N, 15.3. ESMS: *m*/*z* 270 [^{64}Zn(L^{tBu})(NCMe)$_2$]$^+$, 312 [^{64}Zn(L^{tBu})$_2$]$^+$, 353 [^{64}Zn(L^{tBu})$_2$(NCMe)]$^+$, 394 [^{64}Zn(L^{tBu})$_2$(NCMe)$_2$]$^+$, 417 [^{64}Zn$_2$(L^{tBu})$_2$(NCMe)]$^+$, 457 [^{64}Zn(L^{tBu})$_2$(PF$_6$)]$^+$, 500 [^{64}Zn$_2$(L^{tBu})$_3$]$^+$, 562 [^{64}Zn$_2$(L^{tBu})$_2$(NCMe)(PF$_6$)]$^+$. NMR spectra (CDCl$_3$, 295 K) ^{1}H δ (ppm): 1.27 (54H, CCH_3), 6.16 (d, 2.2 Hz, 6H, Pz H^4), 7.35 (d, 2.2 Hz, 6H, Pz H^3), 9.73 (br s, 6H, NH). {^{1}H}^{13}C δ (ppm): 30.1 (CCH$_3$), 31.8 (CCH$_3$), 103.3 (Pz C^4), 139.7 (Pz C^3), 158.1 (Pz C^5). IR (Nujol): 3402m, 3180m, 3158m, 3142m, 3082w, 1570w, 1555m, 1491m, 1340w, 1304m, 1263m, 1208m, 1179w, 1125s, 1090m, 1073w, 996m, 962m, 929m, 847s br, 798m, 740w, 722m, 665w, 644w cm^{-1}. IR (CD_2Cl_2): 3470m, 3408m cm^{-1}. While **4** can be stored in air at room temperature, heating to 60 °C in air leads to loss of crystallinity, which yields a sticky white solid that analyzed approximately as the monohydrate of **4** (*cf.* **5** below): found C, 44.7; H, 6.5; N, 15.0. Anal. Calcd for $C_{42}H_{72}F_{12}N_{12}P_2Zn·H_2O$: C, 45.1; H, 6.7; N, 15.0.

Table 1. Crystallographic Data for **1**, **3**, and **4**

	1	**3**	**4**
formula	$C_{28}H_{48}N_{10}O_6Zn$	$C_{56}H_{96}Cl_2N_{16}O_8Zn$	$C_{42}H_{72}F_{12}N_{12}P_2Zn$
fw	686.13	1257.76	1100.43
crystal syst	orthorhombic	triclinic	hexagonal
space group	*Pbcn*	$P\bar{1}$	$P3_22_1$
a (Å)	10.2597(5)	13.2821(1)	10.2487(1)
b (Å)	19.9558(11)	13.2855(2)	
c (Å)	18.0052(9)	20.8585(3)	45.1513(5)
α (°)		87.2741(4)	
β (°)		72.4221(5)	
γ (°)		89.6037(5)	
V (Å^3)	3686.4(3)	3504.74(8)	4107.13(7)
Z	4	2	3
T (K)	150(2)	150(2)	150(2)
D (g·cm^{-3})	1.236	1.192	1.335
F(000)	1456	1344	1728
λ (Å)	0.71073	0.71073	0.71073
μ (mm^{-1})	0.716	0.485	0.589
total data collected	77963	71569	25512
independent reflections	4474	16056	6252
R_{int}	0.032	0.073	0.074
R, R_w [$I > 2\sigma(I)$]	0.058, 0.156	0.060, 0.165	0.050, 0.136
R, R_w [all data]	0.071, 0.170	0.083, 0.184	0.070, 0.149
Flack parameter			−0.022(13)

For **5**, found: C, 38.5; H, 5.6; N, 12.9. Anal. Calcd for $C_{42}H_{72}F_{12}N_{12}Sb_2Zn·H_2O$: C, 38.8; H, 5.7; N, 12.9. ESMS: *m*/*z* 270 [^{64}Zn(L^{tBu})(NCMe)$_2$]$^+$, 312 [^{64}Zn(L^{tBu})$_2$]$^+$, 353 [^{64}Zn(L^{tBu})$_2$(NCMe)]$^+$, 394 [^{64}Zn(L^{tBu})$_2$(NCMe)$_2$]$^+$, 417 [^{64}Zn$_2$(L^{tBu})$_2$(NCMe)]$^+$, 477 [^{64}Zn$_2$(L^{tBu})$_2$(NCMe)$_2$F]$^+$, 500 [^{64}Zn$_2$(L^{tBu})$_3$]$^+$, 588 [^{64}Zn(L^{tBu})$_2$(NCMe)(SbF$_6$)]$^+$, 652 [^{64}Zn$_2$(L^{tBu})$_2$(NCMe)(SbF$_6$)]$^+$, 816 [^{64}Zn$_3$(L^{tBu})$_3$(OH)(SbF$_6$)$_2$]$^+$, 898 [^{64}Zn$_3$(L^{tBu})$_3$(OH)(NCMe)$_2$(SbF$_6$)$_2$]$^+$. NMR spectra (CDCl$_3$, 295 K) ^{1}H δ (ppm): 1.24 (54H, CCH_3), 6.14 (br s, 6H, Pz H^4), 7.47 (br s, 6H, Pz H^3), 11.13 (br s, 6H, NH). {^{1}H}^{13}C δ (ppm): 30.2 (CCH$_3$), 31.7 (CCH$_3$), 103.2 (br, Pz C^4), 138.3 (br, Pz C^3), 157.7 (br, Pz C^5). IR (Nujol): 3383m, 3180m, 3156m, 3144m, 3092m, 1555m, 1492m, 1340w, 1302m, 1261m, 1208m, 1171w, 1124s, 1090m, 1073w, 994m, 962m, 929m, 891w, 803s, 726m, 663s br, 643w cm^{-1}. IR (CD_2Cl_2): 3470m, 3367m cm^{-1}.

Single Crystal X-ray Structure Determinations. Single crystals of **1**, **3**, and **4** were all obtained from solutions of the compounds in CH$_2$Cl$_2$/pentane solvent mixtures at 5 °C. Experimental details from the structure determinations in this work are given in Table 1. Diffraction data from **1** were measured using a Bruker X8 Apex diffractometer with graphite-monochromated Mo Kα radiation (λ = 0.71073 Å) generated by a rotating anode. Data from **3** and **4** were collected on a Nonius Kappa charge-coupled device (CCD) area detector diffractometer, which used graphite-monochromated Mo-K_α radiation from a sealed tube source. Both diffractometers were fitted with Oxford Cryostream low-temperature devices. All structures in this study were solved by direct methods (*SHELXS96*[28]) and developed by full least-squares refinement on F^2 (*SHELXL96*[29]). All figures were prepared using XSEED,[30] which incorporates POVRAY.[31] Details of the structure determinations of [Zn(L^{Mes})$_4$][ClO$_4$]$_2$·2CHCl$_3$ and [Cu(L^{Mes})$_4$][BF$_4$]$_2$·(C$_2$H$_5$)$_2$O are given in the Supporting Information.

X-ray Structure Determination of [Zn(L^{tBu})$_4$][NO$_3$]$_2$ (1). The asymmetric unit contains half a formula unit with Zn(1) lying on the crystallographic C_2 axis [1/2, *y*, 1/4]. The NO$_3^-$ anion is disordered and was modeled over three equally occupied sites labeled A, B, and C. The restraints N−O = 1.26(2) Å and O···O = 2.18(2) Å were applied to this anion. Both *tert*-butyl groups in

---

(28) Sheldrick, G. M. *Acta Crystallogr., Section A* **1990**, *A46*, 467.

(29) Sheldrick, G. M. *SHELXL 97, Program for the Refinement of Crystal Structures*; University of Göttingen: Göttingen, Germany, 1997.

(30) Barbour, L. J. *J. Supramol. Chem.* **2003**, *1*, 189.

(31) *POVRAY* v. 3.5, Persistence of Vision Raytracer Pty. Ltd. http://www.povray.org. Williamstown, Victoria, Australia, 2002.

the model were also disordered and were modeled over three equally occupied sites labeled A, B, and C. The restraints C−C = 1.53(2) Å and 1,3-C···C = 2.50(2) Å were applied to these residues. All wholly occupied non-H atoms were refined anisotropically, and all H atoms were placed in calculated positions and refined using a riding model. Because all the methyl groups are disordered, their torsions were fixed at idealized values. The highest residual Fourier peak of +1.7 e·Å^{-3} lies on the crystallographic C_2 axis [1, *y*, 1/4] and is not bonded to any other atom. There are no other residual Fourier peaks or holes >± 1.0 e·Å^{-3}.

X-ray Structure Determination of [{Zn(L^{tBu})$_4$}(L^{tBu})$_4$][ClO$_4$]$_2$ (3). The asymmetric unit contains one [Zn(L^{tBu})$_4$]$^{2+}$ dication, four molecules of L^{tBu}, and two perchlorate anions. Two *tert*-butyl groups from Zn-coordinated L^{tBu} residues are disordered with each over two orientations labeled A and B with a refined 0.63:0.37 occupancy ratio. All disordered C−C bonds were restrained to 1.53(2) Å and nonbonded 1,3-C···C distances within a given disorder orientation were restrained to 2.50(2) Å. Both ClO$_4^-$ anions also are disordered over three orientations labeled A, B and C. The three complete partial sites for one of these anions were modeled with equal occupancies of 0.33. For the other, three sets of partial O atoms with occupancies of 0.40:0.40:0.20 were used, sharing a common wholly occupied Cl atom. All disordered Cl−O bonds were restrained to 1.42(1) Å and O···O distances within a given partial ClO$_4^-$ moiety to 2.32(1) Å. All non-H atoms of occupancy >0.5 were refined anisotropically, and all H atoms were placed in calculated positions and refined using a riding model.

X-ray Structure Determination of [{Zn(L^{tBu})$_4$}(L^{tBu})$_2$][PF$_6$]$_2$ (4). The asymmetric unit contains half a formula unit with Zn(1) lying on the crystallographic C_2 axis [*y*, *x*, −*z*]. The PF$_6^-$ anion is disordered and was modeled over two sites labeled A and B with refined occupancies of 0.54:0.46. The restraints P−F = 1.58(2) Å and trans-F···F = 3.16(2) Å were applied to this anion. Two of the three *tert*-butyl groups in the model also were clearly disordered and were modeled over two sites labeled A and B. One of these had a refined occupancy ratio of 0.64:0.36, while the other yielded a ratio of 0.54:0.46 (the same as the anion). The restraints C−C = 1.52(2) Å and 1,3-C···C = 2.48(2) Å were applied to these residues. All non-H atoms with occupancies >0.5 as well as the minor anion P environment were refined anisotropically. All H atoms were placed in calculated positions and refined using a riding model. The torsions on crystallographically ordered methyl groups were allowed to refine freely, while those of the disordered methyl groups were fixed.

Results

Treatment of hydrated Zn[NO$_3$]$_2$ and Zn[BF$_4$]$_2$ with 4 equiv of L^{tBu} in MeOH yielded colorless solutions that gave solid residues upon evaporation to dryness. Dissolution of the residue in the minimum volume of CH$_2$Cl$_2$ followed by the addition of ca. 5-fold excess of pentane yielded colorless crystals of [Zn(L^{tBu})$_4$]X$_2$ (X$^-$ = NO$_3^-$, **1**; X$^-$ = BF$_4^-$, **2**). In contrast, similar reactions using Zn[ClO$_4$]$_2$·6H$_2$O or Zn[PF$_6$]$_2$ and Zn[SbF$_6$]$_2$ (generated in situ from ZnCl$_2$ and 2 equiv of the appropriate silver(I) salt) yielded colorless crystalline products whose microanalyses implied that they contained a higher L^{tBu}/Zn mole ratio, which is consistent with the formulas [{Zn(L^{tBu})$_4$}(L^{tBu})$_4$][ClO$_4$]$_2$ (**3**) and [{Zn(L^{tBu})$_4$}(L^{tBu})$_2$]Y$_2$ (Y$^-$ = PF$_6^-$, **4**; Y = SbF$_6^-$, **5**; Chart 2). These unexpected formulations were confirmed by crystallographic structure analyses of **1**, **3**, and **4**. Yields of **3**−**5** were improved by performing the complexations using the appropriate stoichiometry of L^{tBu}, which typically gave the compounds in 30−50% yields. Reaction of Zn[NO$_3$]$_2$ and Zn[BF$_4$]$_2$ with excess L^{tBu} under these conditions still afforded **1** and **2** with the remaining fraction of pyrazole staying in solution. Crystalline **4** was stable in air at room temperature but became hygroscopic upon heating to 60 °C. Compound **5** was less stable, decomposing similarly to a sticky white solid upon direct exposure to air at room temperature. Both decomposition products analyzed approximately as the monohydrates of **4** and **5**. Although crystals of **5** suffer from twinning, because they have the same formulation, hexagonal crystal morphology and hygroscopic nature as **4**, the two compounds are likely to be isostructural.

Chart 2. Structures of the Supramolecular Compounds **3** and **4**[a]

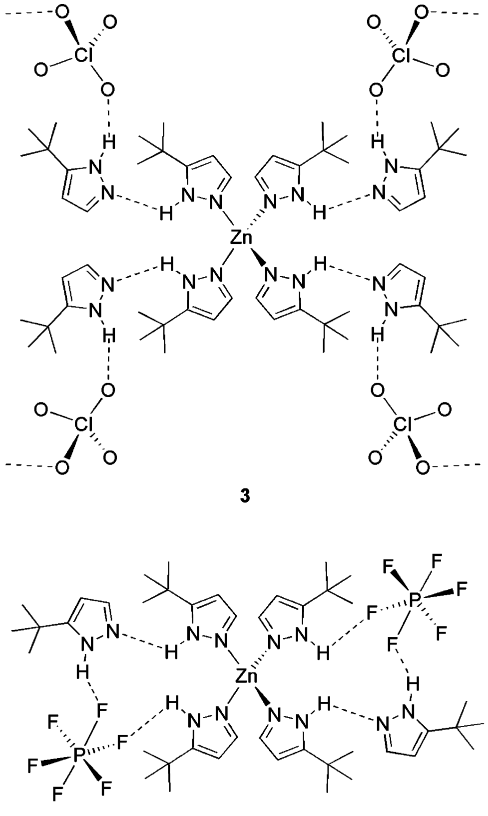

3

4

[a] Compound **5** has the same stoichiometry and hexagonal crystal habit as **4** and is probably isostructural with it.

The zinc center in **1** lies on a crystallographic C_2 axis and has a slightly distorted tetrahedral geometry (Figure 1, Table 2) with individual bond angles at Zn(1) spanning the range 103.31(10)−114.43(13)°. The disordered NO$_3^-$ ion hydrogen bonds to both unique pyrazole ligands through either two or three O atoms depending on the disorder site (Chart 3). Interestingly, the anion also appears to form a $\pi-\pi$ interaction with the symmetry-related pyrazole ring N(2^i)−C(6^i) (Figure 1). The least-squares planes of the three partial nitrate sites and the pyrazole group have dihedral angles between them of 7.0(6)−16.1(5)° and mean interplanar spacings of 3.26(3)−3.53(4) Å. The two interacting moieties lie almost on top of each other with the centroids of the pyrazole ring

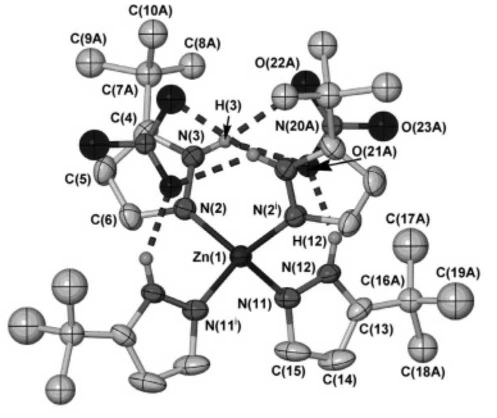

Figure 1. View of the $[Zn(L^{tBu})_4][NO_3]_2$ moiety in the crystal structure of **1** showing the atom numbering scheme employed. For clarity, only the major A orientation of the disordered *tert*-butyl groups and NO_3^- ion are shown, while all C-bound H atoms have been omitted. Thermal ellipsoids are at the 50% probability level except for H atoms, which have arbitrary radii. Symmetry code: (i) $1 - x, y, 1/2 - z$.

Table 2. Selected Bond Lengths (Å) and Angles (deg) for $[Zn(L^{tBu})_4][NO_3]_2$ (**1**) and $[\{Zn(L^{tBu})_4\}(L^{tBu})_2][PF_6]_2$ (**4**)[a]

	1	**4**
Zn(1)−N(2)	2.004(2)	1.995(2)
Zn(1)−N(11)	2.021(2)	1.992(3)
N(2)−Zn(1)−N(2^{x})	114.43(13)	104.97(15)
N(2)−Zn(1)−N(11)	113.61(10)	126.69(10)
N(2)−Zn(1)−N(11^{x})	103.31(10)	101.95(11)
N(11)−Zn(1)−N(11^{x})	108.76(14)	97.31(14)

[a] Symmetry codes. For **1**: (i) $1 - x, y, 1/2 - z$. For **4**: (iv) $y, x, -z$.

Chart 3. Hydrogen-Bond Motifs Shown by the Three Nitrate Ion Disorder Orientations in **1**

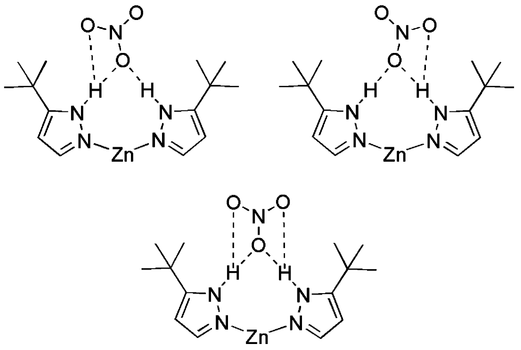

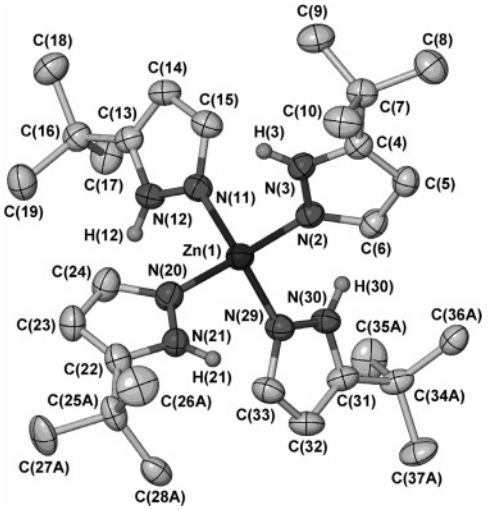

Figure 2. View of the $[Zn(L^{tBu})_4]^{2+}$ moiety in the crystal structure of **3** showing the atom numbering scheme employed. For clarity, only the major A orientations of the disordered *tert*-butyl groups are shown, while all C-bound H atoms have been omitted. Thermal ellipsoids are at the 50% probability level except for H atoms, which have arbitrary radii.

Table 3. Selected Bond Lengths (Å) and Angles (deg) for $[\{Zn(L^{tBu})_4\}(L^{tBu})_4][ClO_4]_2$ (**3**)

Zn(1)−N(2)	1.986(2)
Zn(1)−N(11)	1.989(2)
Zn(1)−N(20)	1.996(2)
Zn(1)−N(29)	1.992(2)
N(2)−Zn(1)−N(9)	106.15(9)
N(2)−Zn(1)−N(15)	116.16(9)
N(2)−Zn(1)−N(20)	107.12(9)
N(2)−Zn(1)−N(27)	105.06(9)
N(2)−Zn(1)−N(33)	116.26(9)
N(9)−Zn(1)−N(15)	106.50(9)

and the three anion sites being offset by only 0.3−0.9 Å. This arrangement presumably affords maximum attraction between the positive dipole on the nitrate N atom and the center of the negative dipole on the pyrazole π-system.

The four Zn(1)−N bonds lengths in the $[Zn(L^{tBu})_4]^{2+}$ center in **3** are equal within experimental error at 1.986(2)−1.992(2) Å, while the average of the bond angles at Zn(1) is exactly equal to the tetrahedral angle at 109.5(2)° (Figure 2 and Table 3). However, the angles N(2)−Zn(1)−N(20) and N(11)−Zn(1)−N(29), which form opposite edges of the tetrahedron, are slightly obtuse at 116.2(9)−116.3(9)°, while the other four N−Zn(1)−N angles are slightly contracted at 105.06(9)−107.12(9)°. Hence, the Zn(II) center in **3** has a slightly flattened tetrahedral geometry. Each pyrazole ligand in **3** hydrogen bonds to another noncoordinated L^{tBu} residue (Chart 2) that affords discrete $[\{Zn(L^{tBu})_4\}(L^{tBu})_4]^{2+}$ supramolecules (Figure 3). The geometries of these four N−H···N hydrogen bonds are all very similar with N···N distances ranging from 2.798(3)−2.818(3) Å and N−H···N angles 165.2−167.3°. The four noncoordinated pyrazole groups in turn donate a hydrogen bond to a (disordered) perchlorate anion, which lies within one of four approximately hemispherical cavities on the surface of the supramolecule that are disposed in an approximately square plane about the zinc center. Each ClO_4^- ion accepts two N−H···O hydrogen bonds from different $[\{Zn(L^{tBu})_4\}(L^{tBu})_4]^{2+}$ supramolecules whose anion-binding pockets combine to encapsulate the anion almost completely (Figure 3). Measurement of the dimensions of the two unique spherical cavities containing the anions is complicated by *tert*-butyl group disorder, but they can be estimated as 5.0 (±0.2) × 5.0 (±0.2) × 4.5 (±0.1) Å. This is slightly larger than the diameter of a ClO_4^- ion (4.4 Å if it is treated as spherical[32]), which accounts for the disorder of the anions within the cavities. The linking of neighboring supramolecules via the ClO_4^- ions by hydrogen bonding leads to a two-dimensional (2D) 4^4 square network in the Schläfli notation[33] running along the (001) crystal plane (see Supporting Information).

---

(32) Mingos, D. M. P.; Rohl, A. L. *J. Chem. Soc., Dalton Trans.* **1991**, 3419.

(33) Carlucci, L.; Ciani, G.; Proserpio, D. M. *Coord. Chem. Rev.* **2003**, *246*, 247.

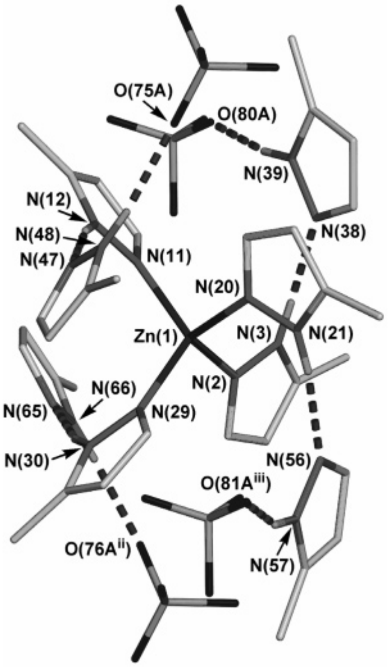

Figure 3. View of the $[\{Zn(L^{tBu})_4\}(L^{tBu})_4]^{2+}$ supramolecule and neighboring ClO_4^- anions in **3** showing the hydrogen bonding interactions involved. For clarity, all C-bound H atoms and *tert*-butyl methyl groups have been omitted and only the major A orientations of the disordered residues in the structure are shown. All atoms have arbitrary radii. Symmetry codes: (ii) x, $1 + y$, z; (iii) $1 + x$, y, z.

Neighboring 4^4 nets interact through van der Waals contacts only.

The $[Zn(L^{tBu})_4]^{2+}$ center in **4** has crystallographic C_2 symmetry with a substantially more flattened coordination geometry than **1** or **3** (Figure 4 and Table 1). The two opposite edges of the tetrahedron are spanned by very obtuse angles [N(2)−Zn(1)−N(11) and its symmetry equivalent] of 126.69(10)°, while the other four angles at Zn(1) have contracted below 109.5° to compensate. The weighted mean of the bond angles at Zn(1) in this compound comes to 109.9(3)°, however, showing that the complex is still best considered as a distorted tetrahedral structure. There is one noncoordinated L^{tBu} molecule in the asymmetric unit (Chart 2), which is oriented almost perpendicular to the other two and is bound to the complex cation by a hydrogen bond donated by N(12)−H(12). This hydrogen bond is slightly longer than the N−H···N interactions in **3**, with N(12)···N(20) = 2.892(3) Å and N(12)−H(12)···N(20) = 161.0°. The disordered PF_6^- anion nestles in a shallow bowl-shaped cavity formed by the faces of the two zinc-bound L^{tBu} ligands. This cavity is capped at one end by the *tert*-butyl group from the hydrogen-bonded L^{tBu} moiety and at the other end by a pyrazole *C3*−H group from the opposite face of the molecule. The anion is held within the bowl by two N−H···F interactions donated by N(3)−H(3) and the unligated pyrazole donor N(21)−H(21) (Figure 5). Unlike in **3**, the PF_6^- ions in **4** do not bridge between complex centers, so **4** crystallizes as discrete $[\{Zn(L^{tBu})_4\}(L^{tBu})_2][PF_6]_2$ moieties.

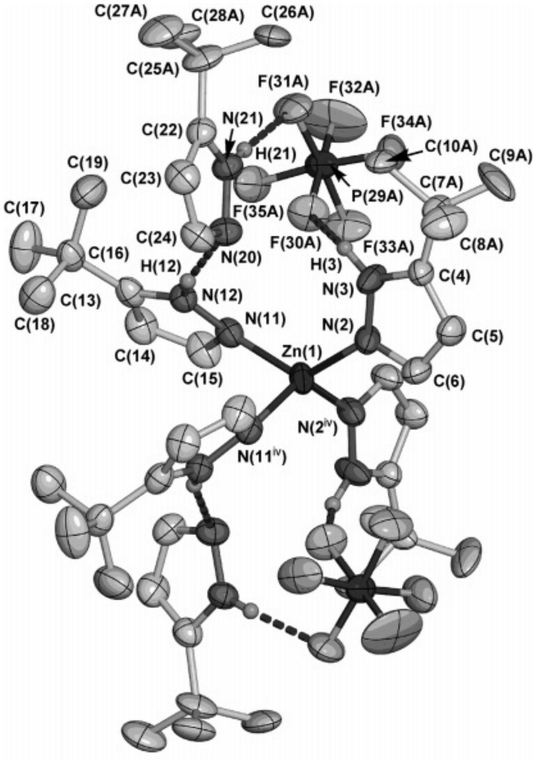

Figure 4. View of the $[\{Zn(L^{tBu})_4\}(L^{tBu})_2]^{2+}$ supramolecule and neighboring PF_6^- anions in **4** showing the atom numbering scheme employed. For clarity, only the major A orientations of the disordered *tert*-butyl groups and PF_6^- ion are shown, while all C-bound H atoms have been omitted. Thermal ellipsoids are at the 50% probability level except for H atoms, which have arbitrary radii. Symmetry code: (iv) y, x, $-z$.

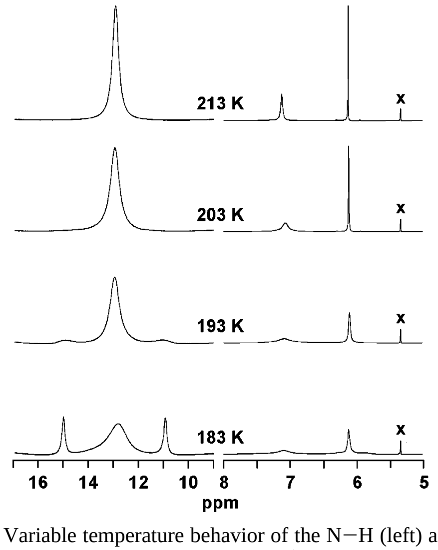

Figure 5. Variable temperature behavior of the N−H (left) and aromatic C−H (right) regions of the 500.13 MHz ^1H NMR spectrum of **3** in CD_2Cl_2.

Comparison of powder diffraction data from **1** and **4** at 150 K with simulations derived from their crystal structures at the same temperature demonstrated that bulk samples of these materials are phase-pure (see Supporting Information). However, data from **3** exhibit two peaks that do not have an obvious match in its simulated diffraction pattern, which suggests that bulk samples of this compound might contain a second minor contaminent phase that we have been unable to identify. To avoid ambiguities, IR and NMR measurements on **3** were performed using individual single crystals, which were hand-picked from a sample of cubic crystals that were ca. 1.5 mm in each dimension. Unfortunately, it was impossible to confirm whether **5** is isostructural with **4** using powder diffraction because of its hygroscopic nature.

All of the ^{1}H and ^{13}C NMR spectra of **1**−**5** in dry $CDCl_3$ show only a single L^{tBu} environment, and they are very similar except for their N−H proton resonance whose chemical shift varies significantly between the compounds. That implies that if the solid-state structures of **3**−**5** are retained in solution the zinc-bound and uncoordinated pyrazole moieties must be in rapid chemical exchange. It also shows that the existence of free and coordinated L^{tBu} in **3**−**5** cannot be simply inferred from the chemical shifts of their NMR spectra. No changes in the NMR spectra of **3** in $CDCl_3$ were apparent upon cooling to 213 K, which is the lowest temperature accessible in this solvent, apart from a downfield migration of the N−H resonance. However, in CD_2Cl_2, the ^{1}H spectrum of **3** broadens significantly upon cooling to 203 K, while at lower temperatures, the resonances from the pyrazole ring C−H protons and the N−H group begin to decoalesce (Figure 5). This decoalescence is <50% complete at 183 K, which is just above the freezing point of the solution. It is clear at 183 K that the broad singlet N−H peak at 12.9 ppm is decoalescing into two similar peaks of equal integral (10.9 and 15.0 ppm) (Figure 5). We assign these peaks to uncoordinated and zinc-bound L^{tBu}, respectively. Because the chemical shift of the former peak is similar to that of free L^{tBu} in this solvent,[7] these data imply that $[\{Zn(L^{tBu})_4\}(L^{tBu})_4]^{2+}$ supramolecule dissociates in CD_2Cl_2 and yields intact tetrahedral $[Zn(L^{tBu})_4]^{2+}$ and 4 equiv of free L^{tBu}. Partial decoalescence of the pyrazole ring ^{13}C NMR resonances from **3** also is evident at 183 K in CD_2Cl_2 (see Supporting Information).

The existence of free and Zn-bound L^{tBu} in CD_2Cl_2 solutions of these compounds also is apparent by IR in that **1**−**5** all show two peaks in the $\nu\{N-H\}$ region: a sharp peak at 3470 cm^{-1} (attributable to free L^{tBu} [34]) and a broader peak in which the position varies between compounds at 3210−3408 cm^{-1} so that we assign it to Zn-bound L^{tBu}. The height of the 3470 cm^{-1} vibration relative to the lower energy peak is a crude indicator of the ratio of free/coordinated pyrazole in the solutions and follows the trend **2** (ca. 1:8) < **1** ≪ **4** ≈ **5** < **3** (ca. 1:1). While this ratio cannot be used to quantitate the compositions of the solutions directly, it is the ordering expected from the stoichiometries of the solid materials. All five solid compounds show a single broad $\nu\{N-H\}$ vibration between 3170 and 3402 cm^{-1} as Nujol mulls. However, the existence of free and coordinated L^{tBu} in solid **3** and **4** is reflected in a splitting of their pyrazole C═C−C═N ring vibration near 1560 cm^{-1} [34,35] into two distinct peaks separated by 15−19 cm^{-1}. Only a single peak is exhibited in this region by **1** and **2**, while **5** (which is likely to be isostructural with **4**) gives one peak but with a pronounced high-energy shoulder.

To test the generality of our results, reactions of $Zn[ClO_4]_2$ and $Zn[PF_6]_2$ with 6−8 mole equiv of other pyrazole derivatives were also attempted using the same procedures as for **3**−**5**. When pyrazole itself was used, salts of the known octahedral complex $[Zn(L^H)_6]^{2+}$ [12,36] were obtained in this way. Similar reactions using 3{5}-methyl-, 3{5}-thienyl-, and 3{5}-*iso*propyl-pyrazole afforded simply intractable oils. However, crystallization of a mixture of $Zn[ClO_4]_2$ and 8 equiv of 3{5}-mesitylpyrazole (L^{Mes}) afforded distinct single crystals of $[Zn(L^{Mes})_4][ClO_4]_2\cdot 2CHCl_3$ and uncoordinated L^{Mes}, which were identified by X-ray diffraction. Interestingly, the zinc center in $[Zn(L^{Mes})_4][ClO_4]_2\cdot 2CHCl_3$ adopts a tetragonal six-coordinate geometry with trans-coordinated ClO_4^- anions (see Supporting Information). This contrasts with the tetrahedral metal centers in **1**, **3**, and **4** but instead, resembles nearly all other crystallographically characterized complexes of the $[M(pz)_4]X_2$ type where M ≠ Zn,[15−23] including $[Cu(L^{Mes})_4][BF_4]_2\cdot(C_2H_5)_2O$ (see Supporting Information). The crystals of metal-free L^{Mes} were isostructural with those previously published for this compound.[37] On this limited evidence, the formation of crystalline supramolecular assemblies of free and zinc-bound pyrazole donors appears to be peculiar to the L^{tBu} ligand.

Conclusions

We have previously noted that metal-bound L^{tBu} can form binding pockets for anion guests through hydrogen-bonding and hydrophobic interactions involving the *tert*-butyl substituents.[3−7] This work extends these capabilities by showing that L^{tBu} building blocks can be linked into anion-binding scaffolds in the solid state by secondary interactions as well as the coordinative bond. The different stoichiometries and structures of **3** and **4** presumably are dictated by their bound anions and imply that this system must respond very sensitively to their different steric and stereochemical requirements. While ClO_4^- and PF_6^- are both near-spherical, the diameter of a PF_6^- ion is 4.6 Å, which is 0.2 Å larger than a ClO_4^- ion.[32] Since the shortest dimension of the anion cavities in **3** is 4.5 ± 0.1 Å, the larger PF_6^- ion is presumably slightly too large to fit within this superstructure. That would account for the different geometry of supramolecular interactions to the anions **4** compared to **3**. While assemblies of free and bound L^{tBu} such as **3** and **4** are novel in metal−pyrazole complex chemistry, they have clear analogies to the structural chemistry of metal-free pyrazoles. These commonly aggregate into cyclic dimers, trimers, or tetramers in the solid and solution phases through the same type of N−H···N hydrogen bonding seen here.[38]

Our synthesis of **3** contrasts with the recent isolation of $[Zn(L^{tBu})_3(OClO_3)]ClO_4$ and $[Zn(L^{tBu})_4][ClO_4]_2$ by Kläui et al.,[34] under similar but not identical conditions to those in this work and using appropriate L^{tBu}/Zn stoichiometries. Clearly, the solution speciation and crystal chemistry of this

---

(34) Chenskaya, T. B.; Berghahn, M.; Kläui, W.; Graf, J.; Frank, W. *J. Mol. Struct.* **2004**, *700*, 157.

(35) Orza, J. M.; García, M. V.; Alkorta, I.; Elguero, J. *Spectrochim. Acta, Part A* **2000**, *56*, 1469.

(36) Anthonisamy, V. S. X.; Murugesan, R. *Mol. Phys.* **1998**, *94*, 269.

(37) Dias, H. V. R.; Wang, X. *Polyhedron* **2004**, *23*, 2533.

(38) Klein, O.; Aguilar-Parrilla, F.; Lopez, J. M.; Jagerovic, N.; Elguero, J.; Limbach, H.-H. *J. Am. Chem. Soc.* **2004**, *126*, 11718 and references therein.

metal/ligand system are particularly complex. For our own part, we have found that **3** is obtained under our conditions even from solutions containing substoichiometric ligand/metal mole ratios albeit in lower yield and purity. Presumably, **3** is less soluble than the two literature compounds in the CH_2Cl_2/pentane solvent mixture used in this work and therefore, it crystallizes preferentially.

The tetrahedral geometry of the $[Zn(L^{tBu})_4]^{2+}$ centers in **1**, **3**, and **4** also deserves comment. These are the first complexes of type $[M(pz)_4X_2]$ with M = Zn to be structurally characterized (the zinc coordination geometry in the literature compound $[Zn(L^{tBu})_4][ClO_4]_2$ was not determined[34]). However, crystal structures of analogous complexes of copper(II),[15,16] nickel(II),[17,18] cobalt(II),[19] iron(II),[20,21] manganese(II),[22] and other transition ions[23] nearly all exhibit trans-six-coordinate structures. Several of these literature compounds contain L^{tBu},[15,17,20] which implies the tetrahedral structures of **1**, **3**, and **4** are not purely a consequence of the steric bulk of the L^{tBu} ligand. On the other hand, the very similar structures of $[Zn(L^{Mes})_4][ClO_4]_2 \cdot 2CHCl_3$ and $[Cu(L^{Mes})_4][BF_4]_2 \cdot (C_2H_5)_2O$ (see Supporting Information) show that $[Zn(pz)_4X_2]$ complexes can adopt tetragonal structures under the appropriate conditions that are essentially identical to those of other metal ions with the same pyrazole ligand. Hence, the tetrahedral nature of **1**, **3**, and **4** probably reflects a subtle combination of steric factors coupled with the increased preference of zinc(II) for tetrahedral over octahedral coordination compared to these other metals.

Acknowledgment. The authors thank David Wright (Institute of Materials Research, University of Leeds) for the powder diffraction measurements and acknowledge financial support by the EPSRC and the University of Leeds.

Supporting Information Available: Additional figures showing the supramolecular assemblies in the crystal structures of **3** and **4**, powder diffraction data, and the low-temperature ^{13}C NMR spectrum of **3**; synthetic data for $[Zn(L^{Mes})_4][ClO_4]_2$ and $[Cu(L^{Mes})_4][BF_4]_2$ and experimental details, metric parameters, and figures for their solvate crystal structures; and, all crystallographic data in CIF format. This material is available free of charge via the Internet at http://pubs.acs.org.

IC052144Q